

On the scale dependence of the fractal dimension for bandlimited 1/f noise

*Original*

On the scale dependence of the fractal dimension for bandlimited 1/f noise / GRIVET TALOCIA, S.. - In: PHYSICS LETTERS A. - ISSN 0375-9601. - STAMPA. - 200:3-4(1995), pp. 264-276. [10.1016/0375-9601(95)00180-B]

*Availability:*

This version is available at: 11583/1401336 since:

*Publisher:*

Elsevier

*Published*

DOI:10.1016/0375-9601(95)00180-B

*Terms of use:*

This article is made available under terms and conditions as specified in the corresponding bibliographic description in the repository

*Publisher copyright*

(Article begins on next page)

# On the Scale Dependence of Fractal Dimension for Band-limited $1/f^\alpha$ Noise

S. Grivet Talocia \*

*NASA/Goddard Space Flight Center, Code 912, Greenbelt, MD, 20771, USA.*

24 April 1995

*Physics Letters A* 200 (1995) 264-276

## Abstract

An analytic approach for the evaluation of the fractal dimension is presented and applied to band-limited  $1/f^\alpha$  noise. High and low cutoff frequencies are shown to affect the scaling exponent, which is time-scale dependent. Asymptotic expansions of the fractal dimension are derived and compared to numerical estimations.

**Keywords:**  $1/f^\alpha$  noise. Fractal dimension. Structure functions. Self-affinity.

---

\*Additional affiliation: Science Systems and Applications, Inc. (SSAI), 5900 Princess Garden Parkway, Lanham, MD, 20706, USA. E-mail: grivet@omar.gsfc.nasa.gov, fax: (301)286-1762.

# 1 Introduction

The ubiquity of processes with  $1/f^\alpha$  spectrum is well established. When looked at in the time domain, these signals are very irregular and present details in a wide range of time scales. This is the main reason that the interest in their fractal characterization has been growing during the last years. The fractal geometry is indeed a natural framework for the description of jagged and crinkled curves, as pointed out by Mandelbrot [1].

The main observable which can be associated with a fractal object (hereafter we will indicate with fractal object a curve lying in the plane) is the fractal dimension  $D$  [2], a quantitative measure of its space-filling properties. The fractal dimension is usually defined [3] as the scaling exponent of the number of  $\epsilon$ -balls needed to cover the set with their radius. If the curve is the graph of a function, as in the case of a time series, another parameter can be used to describe its structure, the exponent  $H$ , which is associated with the scaling of the structure functions of the time-delayed signal (see Section 2). It can easily be shown [4] that this exponent is related to the fractal dimension through  $D = 2 - H$ , and to the spectral logarithmic slope through  $\alpha = 1 + 2H$ . The latter expression has been widely used in modelling the fractional Brownian motion since the work of Mandelbrot [5].

Thereafter, the fractal dimension has been proposed as an alternative tool for the description of  $1/f^\alpha$  signals [6]. The main problem arising from this approach is that numerical estimations of fractal dimension are generally biased, even if many algorithms have been proposed and used so far [7, 8, 9].

A recent paper by Theiler [10] has addressed the problem of the evaluation of the correlation dimension for  $1/f^\alpha$  processes, introducing low and high frequency cutoffs to ensure that the total power does not diverge to infinity. Moreover they are intrinsic in every finite-length and sampled time series. As an intermediate result, Theiler evaluated the theoretical exponent  $H$  in three different scaling regimes induced by the limited band of the signal.

In this work we will consider the same process with a band-limited  $1/f^\alpha$  power spectrum, and will further investigate its fractal properties. We will show that the exponent  $H(T)$ , which describes the scaling of the signal in a restricted time scales range, is not constant with  $T$ , because of corrective terms due to the frequency cutoffs. The zeroth order approximation coincides with the values obtained by Theiler. Higher order asymptotic expansions of  $H(T)$  will be found for values of  $\alpha \in (0, 4)$ , and will be compared to numerical estimates. Our results explain the discrepancies between theoretical models and numerical results found by Fox [7] and Higuchi [8], and can be used to correct the raw biased estimates of the scaling exponents.

## 2 Evaluation of the scaling exponents

### 2.1 Power Spectrum and $H(T)$

We consider a continuous process  $x_t$ , characterized by a power spectrum  $P(f)$ . The exponent  $H$  is defined (see Ref. [11], or Ref. [2] with other notations) as

$$\sigma_T^2 = \langle |x_t - x_{t-T}|^2 \rangle \sim T^{2H}, \quad (1)$$

and describes quantitatively the degree of irregularity of the curve  $(t, x_t)$ . The quantity  $\sigma_T^2$  is called (second order) structure function [12]. Even if many models have been proposed for generating and describing multi-affine curves (see Refs. [13, 14] and Ref. [12] for applications to geophysical data), we will concentrate on mono-affine fractals (i.e. fractional Brownian motion traces), for which the  $q$ th order structure function has a linear scaling exponent with respect to  $q$ :  $\langle |x_t - x_{t-T}|^q \rangle \sim T^{qH}$ . This allows us to link the spectral slope (related to the second order structure function) and the graph dimension (related to the first order one) to the only parameter  $H$ .

The allowed values for the exponent are  $0 \leq H \leq 1$ . If  $H \rightarrow 0$  the  $\sigma_T$  statistic does not depend on  $T$  and the process is delta-correlated. If  $H \rightarrow 1$  the process is smooth, while in the case  $H = 1/2$  we have a mono-dimensional random walk. Mandelbrot and Van Ness [5] introduced this exponent to characterize fractional Brownian motion, and showed that the corresponding power spectrum scales with frequency according to  $1/f^\alpha$ . The relation between  $\alpha$  and  $H$  is well known:

$$\alpha = 1 + 2H. \quad (2)$$

As noted by Theiler [10] a pure  $1/f^\alpha$  spectrum is physically impossible, because the total power of the process would be infinite. Therefore it is necessary to introduce a low frequency cutoff  $f_0$  and a high frequency cutoff  $f_1$  in order to describe real signals (we will assume  $f_0 \ll f_1$  to insure a sufficiently long scaling range). These two cutoff frequencies can be introduced explicitly with bandpass filtering, but every real time series has implicit frequency cutoffs, due to finite length and sampling. This case will be discussed in section 3.

We will consider hereafter a signal characterized by a power spectrum given by:

$$\begin{aligned} P(f) &= f_0^{-\alpha}, & f \leq f_0, \\ &= f^{-\alpha}, & f_0 < f < f_1, \\ &= 0, & f \geq f_1. \end{aligned} \quad (3)$$

This insures that the variance is finite and well defined:

$$\langle x_t^2 \rangle = \int_0^\infty P(f) df < \infty. \quad (4)$$

Given the power spectrum (3), it is straightforward to write an expression for the variance  $\sigma_T^2$  of the delayed signal. We have:

$$\sigma_T^2 = \langle (x_t - x_{t-T})^2 \rangle = 2\langle x_t^2 \rangle - 2\langle x_t x_{t-T} \rangle = 2\langle x_t^2 \rangle [1 - A(T)], \quad (5)$$

where  $A(T)$  is the autocorrelation function of the process, and can be expressed as the inverse Fourier transform of the power spectrum. The expression for  $\sigma_T^2$  is then:

$$\sigma_T^2 = 4 \int_0^\infty P(f) \sin^2(\pi f T) df = 2f_0^{1-\alpha} \left( 1 - \frac{\sin(2\pi f_0 T)}{2\pi f_0 T} \right) + 4 \int_{f_0}^{f_1} f^{-\alpha} \sin^2(\pi f T) df. \quad (6)$$

The asymptotic behavior of  $\sigma_T$  has been evaluated by Theiler [10], using the same model of the spectrum. He showed that

$$\begin{aligned} \sigma_T &\sim T, & T \ll 1/f_1, \\ &\sim T^{\frac{\alpha-1}{2}}, & 1/f_1 \ll T \ll 1/f_0, \\ &\sim \text{const}, & T \gg 1/f_0, \end{aligned} \quad (7)$$

from which the correct fractal scaling can be noted in the intermediate time range. From these expressions we can see that the exponent  $H$  is dependent on the time  $T$ , and cannot be considered a global measure over all time scales. Moreover, from (6) we know that, for fixed  $\alpha$ , the relation  $H_\alpha = H_\alpha(T)$  is smooth. In the following we will further investigate this relation, showing that the transition between different scaling regimes affects the evaluation of the exponent  $H$ . To emphasize the time-scale dependence, we define the function  $H(T)$  as the logarithmic derivative of  $\sigma_T$ :

$$H(T) = \frac{T}{2\sigma_T^2} \cdot \frac{d}{dT} \sigma_T^2. \quad (8)$$

This can be interpreted as the local slope of  $\sigma_T$  when plotted in a double logarithmic plot (a similar definition was introduced by Higuchi [8]). The scale dependence of the fractal dimension can be easily obtained through  $D(T) = 2 - H(T)$ , so we will restrict our attention to the exponent  $H(T)$ . In the following we will evaluate the function  $H(T)$  in the three different regimes investigated by Theiler ( $T \ll 1/f_1$ ,  $1/f_1 \ll T \ll 1/f_0$ ,  $T \gg 1/f_0$ ), and we will show how the two cutoff frequencies introduce corrective terms to the theoretical values

$$\begin{aligned} H &= 0, & 0 < \alpha \leq 1, \\ &= \frac{1}{2}(\alpha - 1), & 1 < \alpha < 3, \\ &= 1, & 3 \leq \alpha < 4. \end{aligned} \quad (9)$$

## 2.2 Short time scales: $T \ll 1/f_1$

The argument of the sine functions in (6) is small, being  $\xi = \pi f T \ll 1$ ,  $\forall f \in [f_0, f_1]$ . Consequently we can approximate the integral using the expansion  $\sin^2 \xi \sim \xi^2 - \xi^4/3$ , and the other term using  $(1 - \sin \xi/\xi) \sim \xi^2/6 - \xi^4/120$ . From (6) we obtain, if  $\alpha \neq 3$ ,

$$\sigma_T^2 \sim \frac{f_1^{1-\alpha}}{3-\alpha}(2\pi f_1 T)^2 - \frac{\alpha f_0^{1-\alpha}}{3(3-\alpha)}(2\pi f_0 T)^2 - \frac{f_1^{1-\alpha}}{12(5-\alpha)}(2\pi f_1 T)^4 + \frac{\alpha f_0^{1-\alpha}}{60(5-\alpha)}(2\pi f_0 T)^4. \quad (10)$$

Taking the logarithmic derivative as indicated in (8) we have

$$\begin{aligned} H(T) &\sim \left( \frac{f_1^{1-\alpha}}{3-\alpha}(2\pi f_1 T)^2 - \frac{\alpha f_0^{1-\alpha}}{3(3-\alpha)}(2\pi f_0 T)^2 - \frac{f_1^{1-\alpha}}{6(5-\alpha)}(2\pi f_1 T)^4 + \frac{\alpha f_0^{1-\alpha}}{30(5-\alpha)}(2\pi f_0 T)^4 \right) \\ &\times \left( \frac{f_1^{1-\alpha}}{3-\alpha}(2\pi f_1 T)^2 - \frac{\alpha f_0^{1-\alpha}}{3(3-\alpha)}(2\pi f_0 T)^2 - \frac{f_1^{1-\alpha}}{12(5-\alpha)}(2\pi f_1 T)^4 + \frac{\alpha f_0^{1-\alpha}}{60(5-\alpha)}(2\pi f_0 T)^4 \right)^{-1}. \end{aligned} \quad (11)$$

This expression can be simplified extracting the theoretical value  $H = 1$ , and considering that  $f_0 \ll f_1$ . The exponent  $H(T)$  then reads

$$H(T) \sim 1 - \frac{3-\alpha}{12(5-\alpha)} \cdot \frac{1}{1 - \frac{\alpha}{3} \left( \frac{f_0}{f_1} \right)^{3-\alpha}} \cdot (2\pi f_1 T)^2. \quad (12)$$

The expression for  $H(T)$  in the case  $\alpha = 3$  can be easily obtained from (12) taking the limit for  $\alpha \rightarrow 3$ ,

$$H_{\alpha \rightarrow 3}(T) \sim 1 - \frac{(2\pi f_1 T)^2}{24 \left[ \frac{1}{3} + \log(f_1/f_0) \right]}. \quad (13)$$

### 2.3 Intermediate time scales: $1/f_1 \ll T \ll 1/f_0$

This is the proper fractal scaling regime. The graph  $(t, x_t)$  is fractal only if  $1 < \alpha < 3$ . If  $\alpha > 3$  the high frequency contribution is too small to crinkle the curve, while if  $\alpha < 1$  the theoretical value of  $H$  saturates at 0. However, we will investigate values of  $\alpha$  ranging from 0 to 4, analyzing the three different cases separately.

- **Case  $1 < \alpha < 3$**

For these values of the parameters the integral in (6) exists even when the integration interval tends to  $(0, \infty)$ . The low and high frequency cutoff contribution can easily be evaluated splitting the integral into

$$\sigma_T^2 = 2f_0^{1-\alpha} \left( 1 - \frac{\sin(2\pi f_0 T)}{2\pi f_0 T} \right) + 4T^{\alpha-1} I_0[\alpha] - I_1 - I_2, \quad (14)$$

where

$$I_0[\alpha] = \int_0^\infty u^{-\alpha} \sin^2(\pi u) du \quad (15)$$

$$I_1 = 4T^{\alpha-1} \int_0^{f_0 T} u^{-\alpha} \sin^2(\pi u) du \quad (16)$$

$$I_2 = 4T^{\alpha-1} \int_{f_1 T}^\infty u^{-\alpha} \sin^2(\pi u) du. \quad (17)$$

The first integral is not dependent on  $T$ , and can be expressed in closed form [15] with the  $\Gamma$  function

$$I_0[\alpha] = -\frac{\Gamma(1-\alpha) \cos((1-\alpha)\frac{\pi}{2})}{2^{2-\alpha} \pi^{1-\alpha}}. \quad (18)$$

This is also the term associated to the proper fractal scaling, while the other terms are corrections depending on  $T$ .

The integral  $I_1$  can be approximated expanding the sine function for small values of the argument

$$I_1 \sim 4T^{\alpha-1} \int_0^{f_0 T} [\pi^2 u^{2-\alpha} - \frac{\pi^4}{3} u^{4-\alpha}] du = \frac{f_0^{1-\alpha}}{3-\alpha} (2\pi f_0 T)^2 - \frac{f_0^{1-\alpha}}{12(5-\alpha)} (2\pi f_0 T)^4. \quad (19)$$

The integral  $I_2$  can be approximated using the identity  $\sin^2 \xi = [1 - \cos(2\xi)]/2$  and integrating by parts. The most significant terms are

$$I_2 \sim 2f_1^{1-\alpha} \left\{ \frac{1}{\alpha-1} + \frac{\sin(2\pi f_1 T)}{2\pi f_1 T} - \alpha \frac{\cos(2\pi f_1 T)}{(2\pi f_1 T)^2} \right\} \quad (20)$$

Substituting (19) and (20) in equation (14) and expanding the first term for small arguments, we find the approximate expression for the variance of the delayed signal,

$$\begin{aligned} \sigma_T^2 \sim & 4T^{\alpha-1} I_0[\alpha] - \frac{\alpha f_0^{1-\alpha}}{3(3-\alpha)} (2\pi f_0 T)^2 + \frac{\alpha f_0^{1-\alpha}}{60(5-\alpha)} (2\pi f_0 T)^4 + \\ & + \frac{2f_1^{1-\alpha}}{1-\alpha} - 2f_1^{1-\alpha} \frac{\sin(2\pi f_1 T)}{2\pi f_1 T}. \end{aligned} \quad (21)$$

Taking the logarithmic derivative as indicated in (8) and extracting the theoretical value  $(\alpha-1)/2$  we obtain the scaling exponent

$$H(T) \sim \frac{\alpha-1}{2} + \left\{ (f_0/f_1)^{\alpha-1} (1 - \cos(2\pi f_1 T)) - \frac{1}{6} \alpha (2\pi f_0 T)^2 + \frac{1}{120} \alpha (2\pi f_0 T)^4 \right\}$$

$$\begin{aligned} & \times \left[ \frac{2}{1-\alpha} \left( \frac{f_0}{f_1} \right)^{\alpha-1} - 2\Gamma(1-\alpha) \sin(\alpha\pi/2) (2\pi f_0 T)^{\alpha-1} - \frac{\alpha}{3(3-\alpha)} (2\pi f_0 T)^2 \right. \\ & \left. + \frac{\alpha}{60(5-\alpha)} (2\pi f_0 T)^4 \right]^{-1} \end{aligned} \quad (22)$$

This is valid if  $1 < \alpha < 3$ ,  $\alpha \neq 2$ . If  $\alpha \rightarrow 2$  the  $\Gamma$  function has a singularity, cancelled by the zero of the sine function. In this case we have

$$H_{\alpha \rightarrow 2}(T) \sim \frac{1}{2} + \frac{(f_0/f_1)(1 - \cos(2\pi f_1 T)) - \frac{1}{3}(2\pi f_0 T)^2 + \frac{1}{60}(2\pi f_0 T)^4}{-2f_0/f_1 + \pi(2\pi f_0 T) - \frac{2}{3}(2\pi f_0 T)^2 + \frac{1}{90}(2\pi f_0 T)^4}. \quad (23)$$

• **Case**  $3 \leq \alpha < 4$

In this case the expression (6) does not converge if the integration interval goes to  $(0, \infty)$  because of the singularity in the origin. The convergence for  $f \rightarrow \infty$  is instead rather fast, so the terms due to high frequency cutoff can be neglected, and therefore we will set  $f_1 = \infty$ . The equation (6) can be rewritten as

$$\sigma_T^2 = 2f_0^{1-\alpha} \left( 1 - \frac{\sin(2\pi f_0 T)}{2\pi f_0 T} \right) + \frac{2f_0^{1-\alpha}}{\alpha-1} - 2f_0^{1-\alpha} I_3, \quad (24)$$

where

$$I_3 = \int_1^\infty u^{-\alpha} \cos(2\pi f_0 T u) du. \quad (25)$$

Integrating by parts the preceding expression twice we get:

$$I_3 = \frac{\cos(2\pi f_0 T)}{\alpha-1} + \frac{2\pi f_0 T \sin(2\pi f_0 T)}{(\alpha-1)(\alpha-2)} - \frac{(2\pi f_0 T)^2}{(\alpha-1)(\alpha-2)} \int_1^\infty u^{2-\alpha} \cos(2\pi f_0 T u) du. \quad (26)$$

This operation has decreased by 2 the order of the singularity in the origin. The last integral can be rewritten as

$$\int_1^\infty u^{2-\alpha} \cos(2\pi f_0 T u) du = \frac{1}{\alpha-3} - 2 \int_1^\infty u^{2-\alpha} \sin^2(\pi f_0 T u) du = \frac{1}{\alpha-3} - 2I_4. \quad (27)$$

It is now possible to extract the low frequency contribution splitting the integral and using Eq. (15)

$$\begin{aligned} I_4 &= \int_0^\infty u^{2-\alpha} \sin^2(\pi f_0 T u) du - \int_0^1 u^{2-\alpha} \sin^2(\pi f_0 T u) du = \\ &= I_0[\alpha-2](f_0 T)^{\alpha-3} - I_5. \end{aligned} \quad (28)$$

Finally the integral  $I_5$  can be approximated expanding the sine function for small arguments (the first order is sufficient), obtaining

$$I_5 \sim \frac{(\pi f_0 T)^2}{5 - \alpha}. \quad (29)$$

Substituting (29), (27) and (25) in equation (24) we find

$$\begin{aligned} \sigma_T^2 \sim & \frac{2f_0^{1-\alpha}}{\alpha - 1} \left\{ 1 - \cos(2\pi f_0 T) + \frac{1}{\alpha - 2} 2\pi f_0 T \sin(2\pi f_0 T) + \frac{(2\pi f_0 T)^2}{(\alpha - 2)(\alpha - 3)} + \right. \\ & \left. - \frac{8\pi^2 I_0[\alpha - 2]}{\alpha - 2} (f_0 T)^{\alpha-1} + \frac{(2\pi f_0 T)^4}{2(\alpha - 2)(5 - \alpha)} \right\} + \\ & + 2f_0^{1-\alpha} \left( 1 - \frac{\sin(2\pi f_0 T)}{2\pi f_0 T} \right). \end{aligned} \quad (30)$$

The argument of the trigonometric functions in (30) is small, so they can be replaced by their fourth order McLaurin polynomials. The final approximated expression for  $\sigma_T^2$  is

$$\sigma_T^2 \sim \frac{\alpha f_0^{1-\alpha}}{3(\alpha - 3)} (2\pi f_0 T)^2 + \frac{\alpha f_0^{1-\alpha}}{60(5 - \alpha)} (2\pi f_0 T)^4 - \frac{16 I_0[\alpha - 2] \pi^2 f_0^{1-\alpha}}{(\alpha - 1)(\alpha - 2)} (f_0 T)^{\alpha-1}. \quad (31)$$

Taking the logarithmic derivative (8) and substituting expression (18) for  $I_0[\alpha - 2]$  we get

$$H(T) \sim 1 + \frac{(3 - \alpha)\Gamma(1 - \alpha) \sin(\alpha\pi/2) (2\pi f_0 T)^{\alpha-3} + [\alpha/60(5 - \alpha)] (2\pi f_0 T)^2}{[\alpha/3(\alpha - 3)] - 2\Gamma(1 - \alpha) \sin(\alpha\pi/2) (2\pi f_0 T)^{\alpha-3} + [\alpha/60(5 - \alpha)] (2\pi f_0 T)^2}. \quad (32)$$

Let us consider now the case  $\alpha \rightarrow 3^+$ . The first two terms in the denominator have simple poles with the same residues. The singularity can then be eliminated expanding these terms for  $\alpha \sim 3$ . The final result is

$$H_{\alpha \rightarrow 3}(T) \sim 1 + \frac{-\frac{1}{2} + \frac{1}{40} (2\pi f_0 T)^2}{\frac{11}{6} + \Psi(1) - \log(2\pi f_0 T) + \frac{1}{40} (2\pi f_0 T)^2}, \quad (33)$$

where  $\Psi$  represents the logarithmic derivative of the  $\Gamma$  function,  $\Psi(z) = d \ln \Gamma(z)/dz$ , and evaluated in  $z = 1$  gives  $\Psi(1) = -\gamma \simeq -0.577215$ . Note that the same result can be obtained taking the limit for  $\alpha \rightarrow 3^-$  in Eq. (22).

• **Case**  $0 < \alpha \leq 1$

In this case the contribution of the low frequency cutoff is small and can be easily evaluated because of the convergence of (6) for  $f \rightarrow 0$ . Expanding to the first order the sine function for small arguments we obtain

$$\sigma_T^2 \sim \frac{2f_1^{1-\alpha}}{1-\alpha} - 2 \int_0^{f_1} f^{-\alpha} \cos(2\pi fT) df - \frac{\alpha f_0^{1-\alpha}}{3(3-\alpha)} (2\pi f_0 T)^2. \quad (34)$$

Using [16]

$$\int_0^\infty f^{-\alpha} \cos(2\pi fT) df = \frac{\Gamma(1-\alpha) \sin(\alpha \frac{\pi}{2})}{(2\pi T)^{1-\alpha}}, \quad (35)$$

we can write

$$\sigma_T^2 \sim \frac{2f_1^{1-\alpha}}{1-\alpha} - 2 \frac{\Gamma(1-\alpha) \sin(\alpha \frac{\pi}{2})}{(2\pi T)^{1-\alpha}} + 2 \int_{f_1}^\infty f^{-\alpha} \cos(2\pi fT) df - \frac{\alpha f_0^{1-\alpha}}{3(3-\alpha)} (2\pi f_0 T)^2. \quad (36)$$

From this expression, integrating by parts, we find the approximate expression for  $\sigma_T^2$ ,

$$\sigma_T^2 \sim \frac{2f_1^{1-\alpha}}{1-\alpha} - 2f_1^{1-\alpha} \Gamma(1-\alpha) \sin(\alpha \frac{\pi}{2}) (2\pi f_1 T)^{\alpha-1} - 2f_1^{1-\alpha} \frac{\sin(2\pi f_1 T)}{(2\pi f_1 T)} - \frac{\alpha f_0^{1-\alpha}}{3(3-\alpha)} (2\pi f_0 T)^2. \quad (37)$$

We can now evaluate the exponent  $H(T)$ ,

$$\begin{aligned} H(T) &\sim \left[ (1-\alpha) \Gamma(1-\alpha) \sin(\alpha \pi/2) (2\pi f_1 T)^{\alpha-1} - \cos(2\pi f_1 T) - \frac{\alpha}{3(3-\alpha)} \left(\frac{f_0}{f_1}\right)^{1-\alpha} (2\pi f_0 T)^2 \right] \\ &\times \left[ \frac{2}{1-\alpha} - 2\Gamma(1-\alpha) \sin(\alpha \pi/2) (2\pi f_1 T)^{\alpha-1} - \frac{\alpha}{3(3-\alpha)} \left(\frac{f_0}{f_1}\right)^{1-\alpha} (2\pi f_0 T)^2 - 2 \frac{\sin(2\pi f_1 T)}{(2\pi f_1 T)} \right]^{-1}. \end{aligned} \quad (38)$$

Let us consider the case  $\alpha \rightarrow 1^-$ . Expanding the different terms in expression (38) like for the case  $\alpha \rightarrow 3^+$  and eliminating the singular terms, we obtain

$$H_{\alpha \rightarrow 1}(T) \sim \frac{1 - \cos(2\pi f_1 T) - \frac{1}{6}(2\pi f_0 T)^2}{-2\Psi(1) + 2 \log(2\pi f_1 T) - \frac{1}{6}(2\pi f_0 T)^2 - 2 \sin(2\pi f_1 T)/(2\pi f_1 T)}, \quad (39)$$

which can be found using the same procedure ( $\alpha \rightarrow 1^+$ ) from Eq. (22).

## 2.4 Long time scales: $T \gg 1/f_0$

Equation (6) can be modified, if  $\alpha \neq 1$ , as

$$\sigma_T^2 = 2f_0^{1-\alpha} \left( 1 - \frac{\sin(2\pi f_0 T)}{2\pi f_0 T} \right) + 2 \frac{f_1^{1-\alpha} - f_0^{1-\alpha}}{1-\alpha} - 2 \int_{f_0}^{f_1} f^{-\alpha} \cos(2\pi f T) df. \quad (40)$$

Integrating by parts we can extract the significant terms,

$$\sigma_T^2 \sim \frac{2f_1^{1-\alpha}}{1-\alpha} - \frac{2\alpha f_0^{1-\alpha}}{1-\alpha} - 2f_1^{1-\alpha} \frac{\sin(2\pi f_1 T)}{2\pi f_1 T} - 2\alpha f_0^{1-\alpha} \frac{\cos(2\pi f_0 T)}{(2\pi f_0 T)^2}. \quad (41)$$

The expression for  $H(T)$  is easily found taking the logarithmic derivative of (41),

$$H(T) \sim \frac{\alpha - 1}{2} \cdot \frac{\alpha f_0^{1-\alpha} \sin(2\pi f_0 T)/(2\pi f_0 T) - f_1^{1-\alpha} \cos(2\pi f_1 T)}{\alpha f_0^{1-\alpha} - f_1^{1-\alpha}}. \quad (42)$$

Expression (42) is valid only if  $\alpha \neq 1$ . The exact expression in the case  $\alpha = 1$  can be derived changing the middle term of (40) into  $2 \log(f_1/f_0)$ , or taking the limit for  $\alpha \rightarrow 1$  in (42). The result is

$$H_{\alpha \rightarrow 1}(T) \sim \frac{\sin(2\pi f_0 T)/(2\pi f_0 T) - \cos(2\pi f_1 T)}{2 \left( 1 + \log \frac{f_1}{f_0} \right)}. \quad (43)$$

## 3 Analysis of finite-length sampled signals

As noted above, any real time series has implicit frequency cutoffs. The high frequency cutoff is due to sampling, and is equal to the Nyquist frequency  $f_1 = 1/2T_c$ , where  $T_c$  is the sampling time. The low frequency cutoff is due to the finite length  $T_{\max}$  of the time series, and is equal to  $f_0 = 1/T_{\max}$ . In this section we will derive the scale-dependent exponent  $H(T)$  for a signal where the time index  $T$  is discrete and can only assume values multiple of the sampling time,  $T = nT_c$ . We will also assume that the series is composed by  $N$  samples, i.e.  $T_{\max} = NT_c$ . The scaling of the variance in this case can be expressed as

$$\sigma_{nT_c} \sim (nT_c)^H. \quad (44)$$

Taking the logarithm we get

$$\log(\sigma_{nT_c}) \sim H \log(nT_c) \quad (45)$$

The scaling exponent cannot be derived as in the previous section with a derivative, but has to be defined as an incremental ratio,

$$H_n = \frac{\log(\sigma_{(n+1)T_c}) - \log(\sigma_{nT_c})}{\log((n+1)T_c) - \log(nT_c)} = \frac{1}{\log(1 + \frac{1}{n})} \log \left[ \frac{\sigma_{(n+1)T_c}}{\sigma_{nT_c}} \right]. \quad (46)$$

Moreover, in this case we can only evaluate  $H_n$  in the intermediate fractal scaling regime  $1 \ll n \ll N$ .

Let us first consider the case  $1 < \alpha < 3$ . The expression for the variance of the delayed series can be derived from Eq. (21) substituting  $T = nT_c$ ,

$$\sigma_n^2 \sim 4(nT_c)^{\alpha-1} I_0[\alpha] - \frac{\alpha f_0^{1-\alpha}}{3(3-\alpha)} \left( \frac{2\pi n}{N} \right)^2 + \frac{\alpha f_0^{1-\alpha}}{60(5-\alpha)} \left( \frac{2\pi n}{N} \right)^4 + \frac{2f_1^{1-\alpha}}{1-\alpha}. \quad (47)$$

Combining (47) and (46) we obtain

$$\begin{aligned} H_n &\sim \frac{1/2}{\log(1 + 1/n)} \\ &\times \log \left\{ \left[ 4((n+1)T_c)^{\alpha-1} I_0[\alpha] - \frac{\alpha f_0^{1-\alpha}}{3(3-\alpha)} \left( \frac{2\pi(n+1)}{N} \right)^2 + \frac{\alpha f_0^{1-\alpha}}{60(5-\alpha)} \left( \frac{2\pi(n+1)}{N} \right)^4 + \frac{2f_1^{1-\alpha}}{1-\alpha} \right] \right. \\ &\times \left. \left[ 4(nT_c)^{\alpha-1} I_0[\alpha] - \frac{\alpha f_0^{1-\alpha}}{3(3-\alpha)} \left( \frac{2\pi n}{N} \right)^2 + \frac{\alpha f_0^{1-\alpha}}{60(5-\alpha)} \left( \frac{2\pi n}{N} \right)^4 + \frac{2f_1^{1-\alpha}}{1-\alpha} \right]^{-1} \right\}. \quad (48) \end{aligned}$$

In this scaling regime we can write  $(n+1)^\beta \sim n^\beta + \beta n^{\beta-1}$  for  $\beta > 1$ , so that

$$\begin{aligned} H_n &\sim \frac{1/2}{\log(1 + 1/n)} \\ &\times \log \left\{ 1 + \left[ 4(T_c)^{\alpha-1} I_0[\alpha] (\alpha-1) n^{\alpha-2} - \frac{\alpha f_0^{1-\alpha}}{3(3-\alpha)} \left( \frac{2\pi}{N} \right)^2 2n + \frac{\alpha f_0^{1-\alpha}}{60(5-\alpha)} \left( \frac{2\pi}{N} \right)^4 4n^3 \right] \right. \\ &\times \left. \left[ 4(nT_c)^{\alpha-1} I_0[\alpha] - \frac{\alpha f_0^{1-\alpha}}{3(3-\alpha)} \left( \frac{2\pi n}{N} \right)^2 + \frac{\alpha f_0^{1-\alpha}}{60(5-\alpha)} \left( \frac{2\pi n}{N} \right)^4 + \frac{2f_1^{1-\alpha}}{1-\alpha} \right]^{-1} \right\}. \quad (49) \end{aligned}$$

The big fraction in the logarithm function is  $O(1/n)$ , so we can expand the two logarithms recalling that  $\log(1 + 1/n) \sim 1/n$ . The final expression for  $H_n$  is

$$H_n \sim \frac{\alpha-1}{2} + \left[ \left( \frac{2}{N} \right)^{\alpha-1} - \frac{\alpha}{6} \left( \frac{2\pi n}{N} \right)^2 + \frac{\alpha}{120} \left( \frac{2\pi n}{N} \right)^4 \right]$$

$$\left[ -\frac{2}{\alpha-1} \left(\frac{2}{N}\right)^{\alpha-1} - 2\Gamma(1-\alpha) \sin(\alpha\pi/2) \left(\frac{2\pi n}{N}\right)^{\alpha-1} - \frac{\alpha}{3(3-\alpha)} \left(\frac{2\pi n}{N}\right)^2 + \frac{\alpha}{60(5-\alpha)} \left(\frac{2\pi n}{N}\right)^4 \right]^{-1}. \quad (50)$$

This expression is the discrete equivalent of (22). Note that if we substitute  $T = nT_c$  directly in (22) we obtain one more term coming from  $\cos(2\pi f_1 T)$ . This term is present only in the continuous case because it is a direct consequence of taking the derivative (8). It is then straightforward to derive  $H_n$  for the other values of  $\alpha$ , eliminating this term and passing to discrete values of time. For  $\alpha \rightarrow 2$  we get, from (23),

$$H_{n,\alpha \rightarrow 2} \sim \frac{1}{2} + \left[ \frac{2}{N} - \frac{1}{3} \left(\frac{2\pi n}{N}\right)^2 + \frac{1}{60} \left(\frac{2\pi n}{N}\right)^4 \right] \left[ -\frac{4}{N} + \pi \left(\frac{2\pi n}{N}\right) - \frac{2}{3} \left(\frac{2\pi n}{N}\right)^2 + \frac{1}{90} \left(\frac{2\pi n}{N}\right)^4 \right]^{-1}. \quad (51)$$

The case  $\alpha \geq 3$  is not modified, because we neglected the high frequency contributions since the beginning. From (32) we obtain

$$H_n \sim 1 + \left[ \frac{\Gamma(4-\alpha) \sin(\alpha\pi/2)}{(\alpha-1)(\alpha-2)} \left(\frac{2\pi n}{N}\right)^{\alpha-3} + \frac{\alpha}{60(5-\alpha)} \left(\frac{2\pi n}{N}\right)^2 \right] \times \left[ \frac{\alpha}{3(\alpha-3)} - \frac{2\Gamma(3-\alpha) \sin(\alpha\pi/2)}{(\alpha-1)(\alpha-2)} \left(\frac{2\pi n}{N}\right)^{\alpha-3} + \frac{\alpha}{60(5-\alpha)} \left(\frac{2\pi n}{N}\right)^2 \right]^{-1}. \quad (52)$$

If  $\alpha \rightarrow 3$  we have, from (33),

$$H_{n,\alpha \rightarrow 3} \sim 1 + \frac{-\frac{1}{2} + \frac{1}{40}(2\pi n/N)^2}{\frac{11}{6} + \Psi(1) - \log(2\pi n/N) + \frac{1}{40}(2\pi n/N)^2}. \quad (53)$$

If  $\alpha < 1$  we have, from (38),

$$H_n \sim \frac{(1-\alpha)\Gamma(1-\alpha) \sin(\alpha\pi/2)(\pi n)^{\alpha-1} - [\alpha/3(3-\alpha)](2/N)^{1-\alpha}(2\pi n/N)^2}{2/(1-\alpha) - 2\Gamma(1-\alpha) \sin(\alpha\pi/2)(\pi n)^{\alpha-1} - [\alpha/3(3-\alpha)](2/N)^{1-\alpha}(2\pi n/N)^2}, \quad (54)$$

while if  $\alpha \rightarrow 1$  we get from (39)

$$H_{n,\alpha \rightarrow 1} \sim \frac{1 - \frac{1}{6}(2\pi n/N)^2}{-2\Psi(1) + 2 \log(\pi n) - \frac{1}{6}(2\pi n/N)^2}. \quad (55)$$

## 4 Numerical results

We considered a sampled process with power-law spectrum (3). There are no explicit low and high cutoff frequencies, so the band is determined, like in the previous section, by sampling and finite length. The time axis is normalized to  $[0, 1]$ , while each time series has  $N = 4096$  samples. These choices lead to a Nyquist frequency equal to  $f_1 = 2048$ , while the lowest frequency is  $f_0 = 1$ . For each value of  $\alpha$  we calculated  $M = 20$  different realizations of the process applying inverse FFT to the spectrum. The phases were considered random variables uniformly distributed in  $[0, 2\pi]$ . Each time series thus obtained has been processed to evaluate the function  $\sigma_T = \langle (x_t - x_{t-T})^2 \rangle^{1/2}$  in the range  $10^{-3} < T < 0.2$ . This is the proper fractal scaling regime. The scale-dependent exponent  $H(T)$  has been obtained with a local linear regression over 3 points of  $\{\log T, \log(\sigma_T)\}$ . Then the mean value and the 95% confidence intervals of  $H(T)$  have been evaluated averaging over the  $M$  realizations. The results show that the asymptotic expansions (Fig. 1) match very well the numerical estimations of  $\langle H(T) \rangle$  (Fig. 2). Fig. 3 shows, for different values of  $\alpha$ , the theoretical values of  $H$ , the asymptotic expansions and the statistics of the numerical estimates.

The very good agreement between asymptotic expansions and numerical estimates of  $H(T)$  suggests that these expansions can be used to correct the numerical estimates, in order to cancel the time-scale dependent bias due to finite length and sampling. Fig. 4 shows the corrected estimates, compared to the theoretical values, for different values of  $\alpha$ . These plots have been obtained, for fixed  $T$ , searching for the value of  $\alpha$  such that the asymptotic expansion  $H_\alpha(T)$  is equal to the numerical estimate  $\hat{H}(T)$ . As the expressions for  $H_\alpha(T)$  are not invertible in  $\alpha$ , the corrected values of  $H(T)$  have been found numerically through an iterative zero-finding procedure [17]. Note that the asymptotic expansions viewed as functions of  $\alpha$ , for  $T$  fixed, are smooth and non-decreasing. This insures the existence and unicity of the solution for the inversion procedure.

We recall that the (global) fractal dimension  $D$  can be shown [4] to be equal to  $D = 2 - H$ . In a recently published work [6] Labate et al. evaluated the fractal dimension  $D$  of signals with  $1/f^\alpha$  spectrum using the Variation algorithm [9]. They found that the relation  $D = D(\alpha)$  does not follow exactly the rule  $D = (5 - \alpha)/2$  but there are deviations for values of  $\alpha$  far from 2. The same problems were encountered by Fox [7] and Higuchi [8] using different algorithms. We tried to explain this fact with our expansions, defining a scale-dependent fractal dimension  $D_\alpha(T) = 2 - H_\alpha(T)$  and plotting it versus  $\alpha$  for fixed values of the parameter  $T$ . We obtained the plot in Fig. 5, which is very similar to the results in Refs. [6, 7, 8]. We suggest then that the deviations of numerical estimates from the theoretical values of the exponent  $H$  or fractal dimension  $D$  are a direct consequence of implicit frequency cutoffs due to the finite length and sampling.

## 5 Conclusions

We presented an analytical approach for the evaluation of the time-scale dependence of the fractal dimension for signals with  $1/f^\alpha$  spectrum. In order to consider signals with finite total power we constrained the spectrum to zero in high frequencies range and to a constant for low frequencies. These cutoff frequencies can be explicitly introduced with bandpass filtering, but are implicit in every finite-length and sampled signal. We showed that these cutoffs introduce corrections to the fractal scaling properties of the curve, and that these deviations are time-scale dependent. Moreover, we used the asymptotic expansions to correct the numerical estimates, showing that the time-scale dependent bias due to finite length and sampling can be easily cancelled.

The corrective terms can also explain why numerical estimates of *global* fractal scaling exponents, like the fractal dimension or the exponent  $H$ , are generally biased. The standard procedure for these estimations is the linear regression in a double logarithmic plot of some measure, varying with the chosen algorithm. The scaling exponent is then the slope of the line providing the best fit to the points. This fitting is generally performed globally over many time scales, losing any information relative to the time dependence of the scaling exponent. We performed a local regression in order to investigate this time-scale dependence, and we found that the numerically evaluated scaling exponent  $H(T)$  matches very well the asymptotic expansions derived in this work. This suggests that some of the numerical problems commonly found in estimating the fractal dimension of time series can be explained with the presence of frequency cutoffs due to the finite length and sampling of the signal.

## Acknowledgements

This work was supported by NASA contract No. NAS5-30950. We are grateful to F. Einaudi and F. Canavero for useful comments and for carefully reading the manuscript. Many thanks also to L. Roberti for fruitful discussions.

## References

- [1] B. B. Mandelbrot, *The fractal geometry of Nature* (Freeman, New York, 1982).
- [2] K. Falconer, *Fractal Geometry* (John Wiley & Sons, 1990).
- [3] M. Barnsley, *Fractals Everywhere* (San Diego, Academic Press, 1988).
- [4] H. O. Peitgen and D. Saupe, *The science of fractal images* (Berlin, Springer Verlag, 1988)
- [5] B. B. Mandelbrot, J. W. Van Ness, *SIAM Rev.* 10 (1968) 422.
- [6] D. Labate, F. Canavero, A. DeMarchi, *Metrologia* 31 (1994) 51.
- [7] C. G. Fox, *Pure Appl. Geophys.* 131 (1989) 211.
- [8] T. Higuchi, *Physica D* 46 (1990) 254.
- [9] B. Dubuc, J. F. Quiniou, C. Roques-Carmes, C. Tricot, S. W. Zucker, *Phys. Rev. A* 39 (1989) 1500.
- [10] J. Theiler J., *Phys. Lett. A* 155 (1991) 480.
- [11] J. Feder, *Fractals* (Plenum, New York, 1988).
- [12] A. Davis, A. Marshak, W. Wiscombe, R. Cahalan, *J. Geophys. Res.* 99 (1994) 8055.
- [13] A. Barabási, T. Vicsek, *Phys. Rev. A* 44 (1991) 2730.
- [14] A. Marshak, A. Davis, R. Cahalan, W. Wiscombe, *Phys. Rev. E* 49 (1994) 55.
- [15] I. S. Gradshteyn, I. M. Ryzhik, *Tables of Integrals, Series, and Products* (Academic Press, 1980).
- [16] W. Magnus, F. Oberettinger, R. P. Soni, *Formulas and Theorems for the Special Functions of Mathematical Physics* (Springer-Verlag, New York, 1966).
- [17] W. H. Press, B. P. Flannery, S. A. Teukolsky, W. T. Vetterling, *Numerical Recipes* (Cambridge University Press, 1986).

Figure 1: Asymptotic expansions of the scaling exponent. Shown are the  $H_\alpha(T)$  curves for different values of  $\alpha$ .

Figure 2: Numerical evaluations of the scaling exponent. Shown are the  $\langle H_\alpha(T) \rangle$  curves for different values of  $\alpha$ .

Figure 3: Scaling exponent  $H_\alpha(T)$ : comparison between numerical estimates (circles) and asymptotic expansions (continuous curves). The dotted lines indicate the 95% confidence intervals of numerical estimations. The dashed lines are the theoretical values  $H(T) = (\alpha - 1)/2$  for  $1 \leq \alpha \leq 3$ ,  $H(T) = 0$  for  $\alpha < 1$  and  $H(T) = 1$  for  $\alpha > 3$ .

Figure 4: Corrected values of  $H_\alpha(T)$  (continuous curves) and theoretical values (dashed curves), for different values of  $\alpha$ .

Figure 5: Scale-dependent fractal dimension  $D_\alpha(T) = 2 - H_\alpha(T)$  obtained from the asymptotic expansions, plotted as a function of spectral slope  $\alpha$  for different time scales  $T = nT_c$ , where  $T_c$  is the sampling time. The total number of samples is  $N = 4096$ . The thick curve represents the theoretical values of (global) fractal dimension:  $D = (5 - \alpha)/2$  for  $1 \leq \alpha \leq 3$ ,  $D = 1$  for  $\alpha > 3$  and  $D = 2$  for  $\alpha < 1$ .

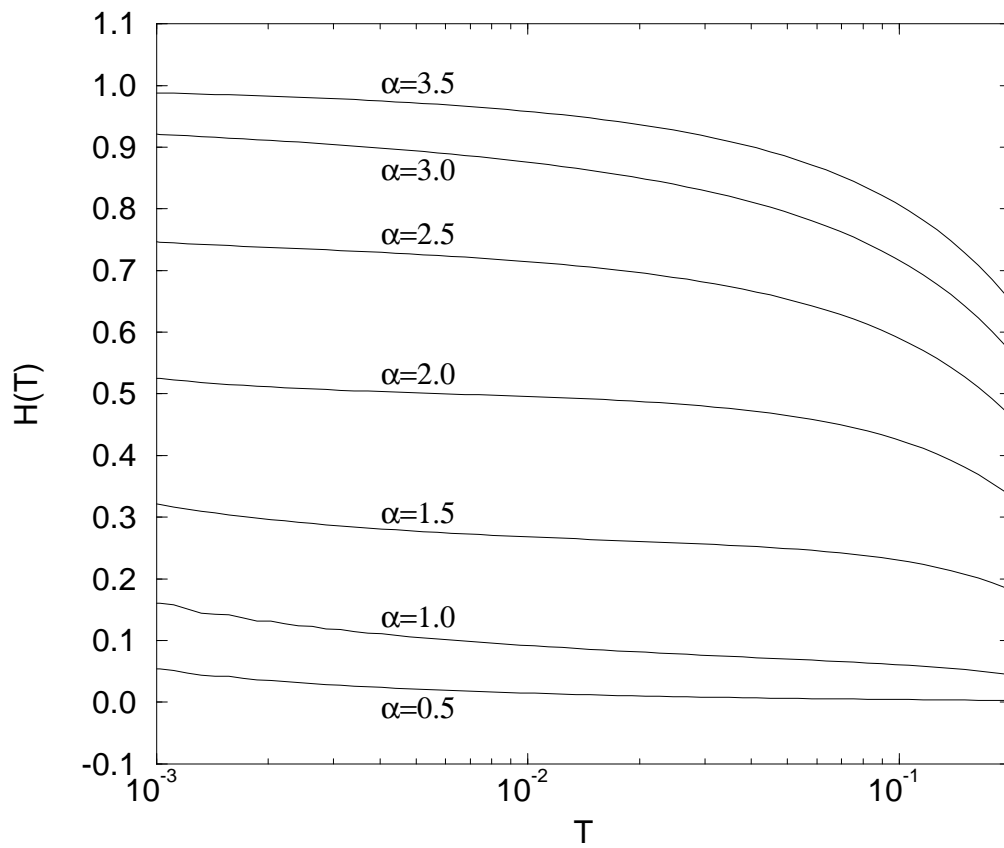


Figure 1

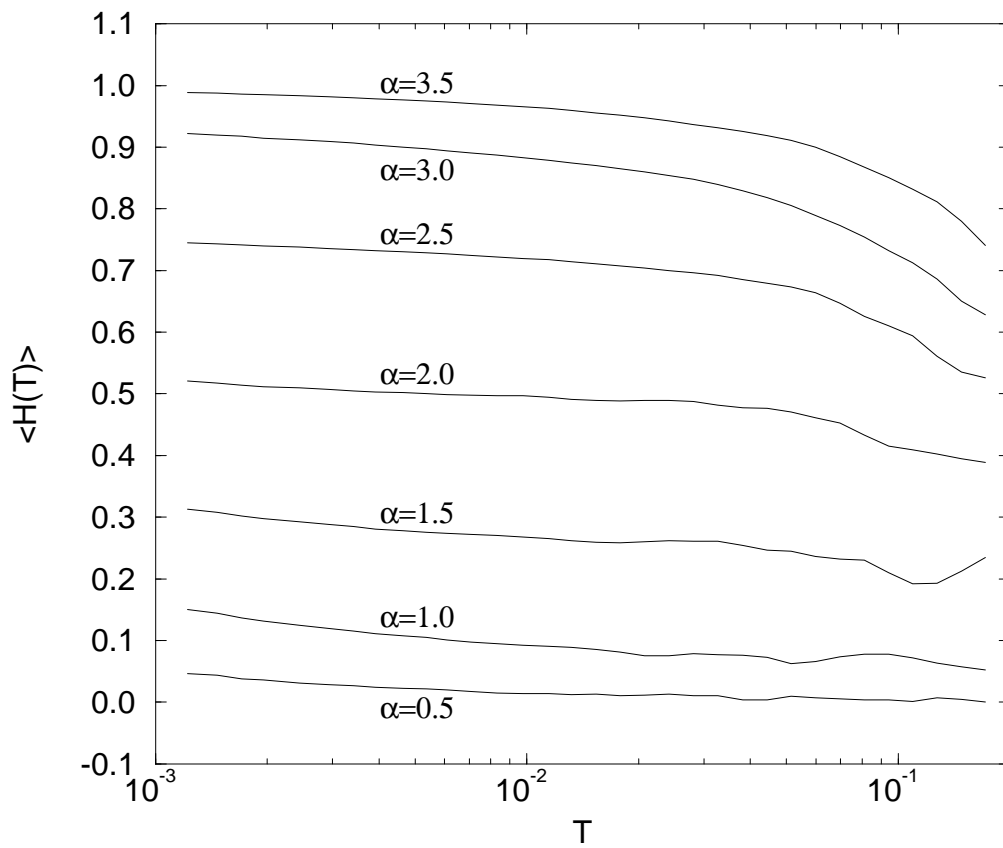


Figure 2

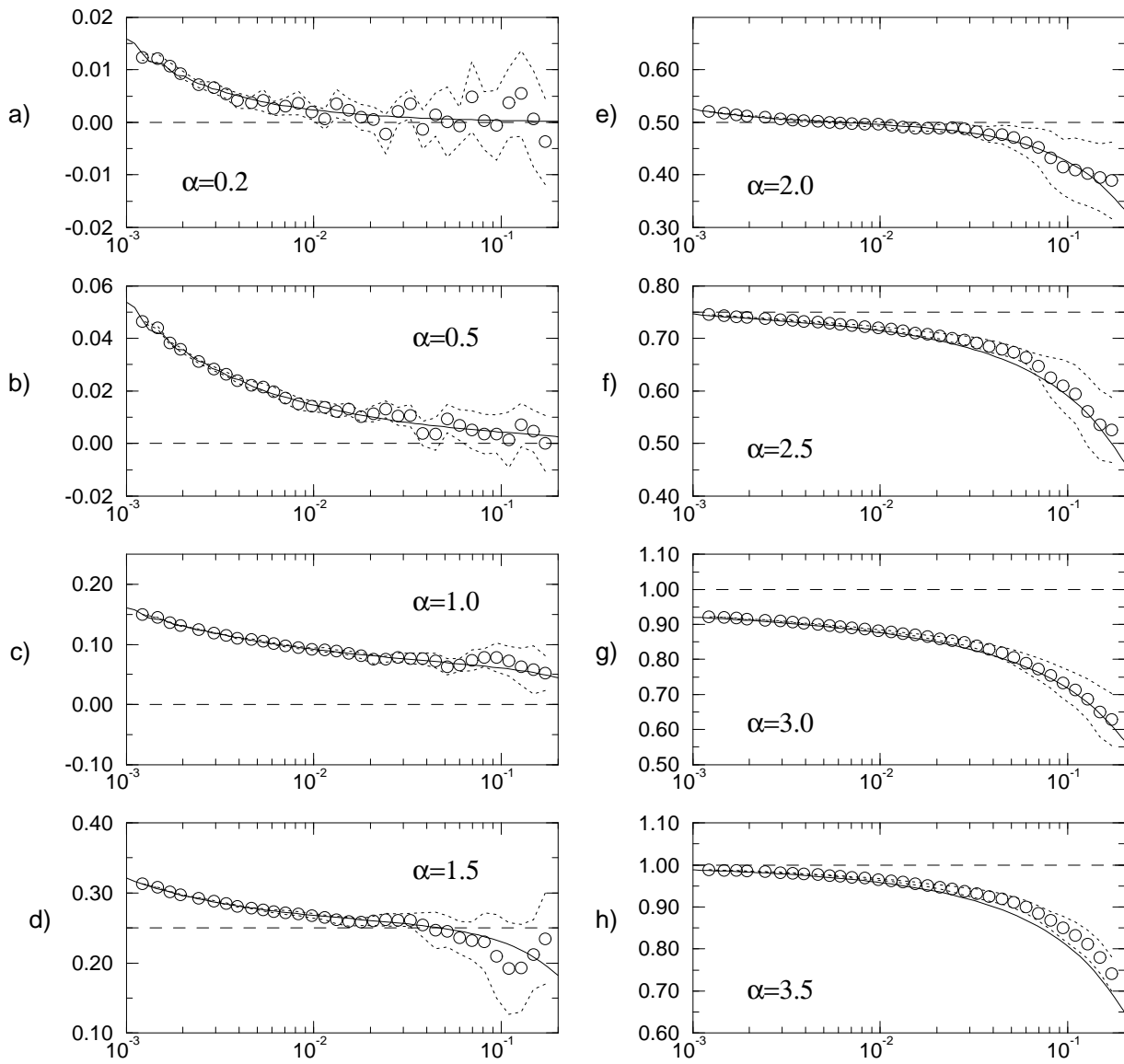


Figure 3

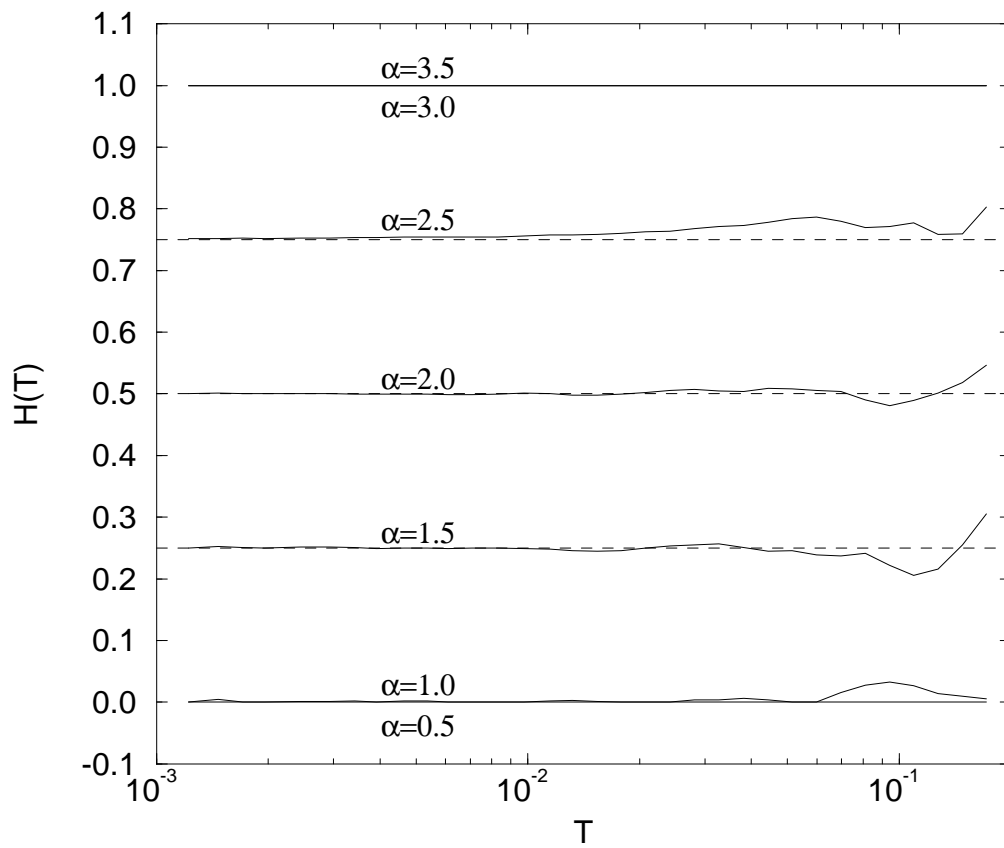


Figure 4

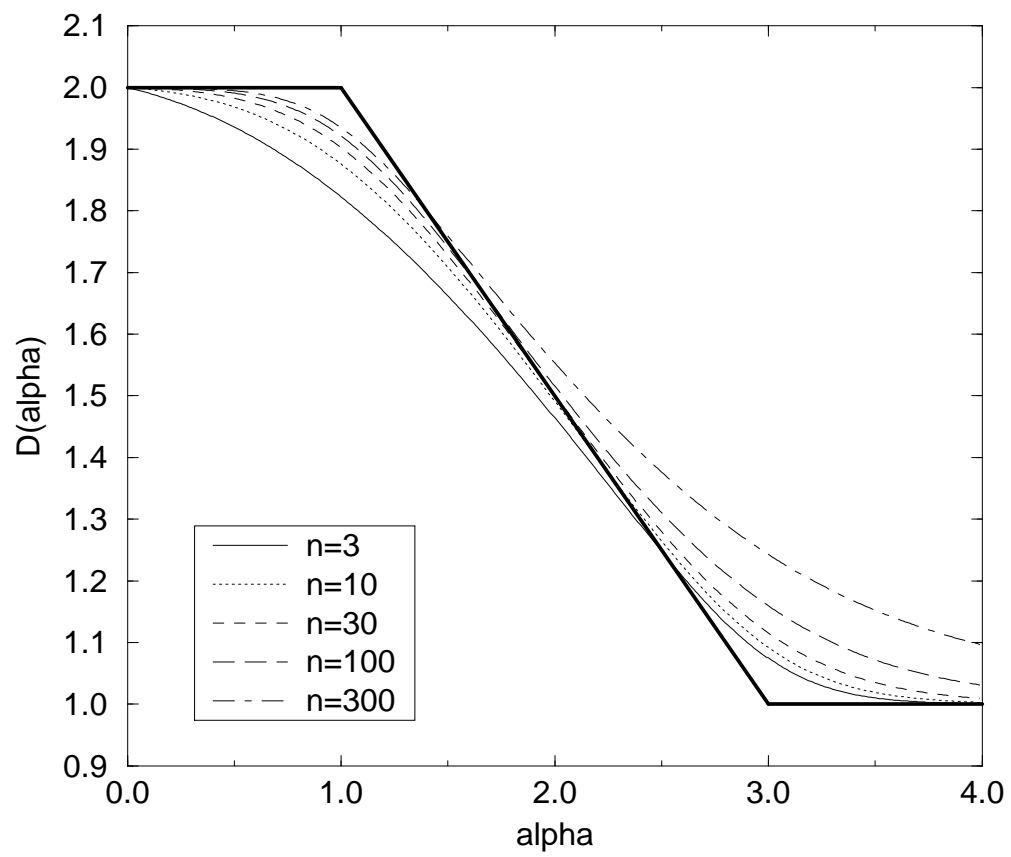


Figure 5